Bohnhoff, M., Bulut, F., Görgün, E., Milkereit, C., Dresen, G. (2008): Seismotectonic setting at the North Anatolian Fault Zone after the 1999 Mw=7.4 Izmit earthquake based on high-resolution aftershock locations. - Advances in Geosciences, 14, 85-92.

Adv. Geosci., 14, 85–92, 2008
www.adv-geosci.net/14/85/2008/

Advances in Geosciences

Seismotectonic setting at the North Anatolian Fault Zone after the 1999 Mw=7.4 Izmit earthquake based on high-resolution aftershock locations

M. Bohnhoff, F. Bulut, E. Görgün, C. Milkereit, and G. Dresen

GeoForschungsZentrum Potsdam, Telegrafenberg D424, 14473 Potsdam, Germany

Received: 15 June 2007 – Revised: 28 September 2007 – Accepted: 4 October 2007 – Published: 2 January 2008

Abstract. The most recent devastating earthquakes that occurred along the North Anatolian Fault Zone (NAFZ) in northwestern Turkey were the 1999 Izmit (Mw=7.4) and Düzce (Mw=7.1) events. In this study we present a catalog of Izmit aftershock hypocenters that was deduced from a network covering the entire 140 km long rupture of the mainshock. 7348 events with a location accuracy better than 5 km are analysed. Aftershocks were observed along the entire ruptured segment along a 20 km wide band of activity. Events are clustered in distinct regions and dominantly occur at 5 to 15 km depth. The eastern termination of the Izmit rupture is characterized by a sharp and steeply dipping boundary exactly where the Düzce mainshock initiated 87 days after the Izmit event. Relocation of the events using double-difference technology results in 4696 high-resolution hypocenters that allow resolving the internal structure of the seismically active areas with a resolution of 300 m (horizontal) and 400m (vertical). Below the Akyazi Plain, representing a small pull-apart structure at a triple junction of the NAFZ, we identify planes of activity that can be correlated with nodal planes of EW extensional normal faulting aftershocks. Along the easternmost Karadere-Düzce segment we identify the down-dip extension of the Karadere fault that hosted about 1 m of right-lateral coseismic slip. At the easternmost rupture we correlate a cloud-type distribution of seismic activity with the largest aftershocks in this area, a subevent of the Izmit mainshock and the Düzce mainshock that all have an almost identical focal mechanism. This part of the NAFZ is interpreted as a classical example of a seismic barrier along the fault.

Correspondence to: M. Bohnhoff
(bohnhoff@gfz-potsdam.de)

1 Tectonic setting

The North Anatolian Fault Zone (NAFZ) represents a 1600 km long plate boundary that slips at an average rate of 20–30 mm/yr (e.g. Barka, 1992; McClusky et al., 2000). It has developed in the framework of the northward moving Arabian plate and the Hellenic subduction zone where the African lithosphere is subducting below the Aegean (see Fig. 1a). Comparison of long-term slip rates with Holocene and GPS-derived slip rates indicate an increasing westward movement of the Anatolian plate with respect to stable Eurasia (Straub et al., 1997; Hubert-Ferrari et al., 2002; Muller and Aydin, 2005). During the last century, the NAFZ has ruptured over 900 km of its length (Ambraseys, 1970; Barka, 1999). A series of large earthquakes starting in 1939 near Erzincan in Eastern Anatolia propagated westward towards the Istanbul-Marmara region in NW Turkey resulting in a $>$100 km long seismic gap below the Sea of Marmara (e.g. Töksöz et al., 1979; Stein et al., 1997; Reilinger et al., 2000). This segment did not rupture since 1766 and is believed being capable of generating two M$\geq$7.4 earthquakes within the next decades (Hubert-Ferrari et al., 2000).

The most recent devastating earthquakes along the NAFZ occurred in 1999 near Izmit and Düzce with magnitudes of 7.4 and 7.1, respectively, (e.g. Tibi et al., 2001; Barka et al., 2002; Aktar et al., 2004) rupturing an almost 200 km long segment (see Fig. 1b). The Izmit event occurred on 17 August 1999 and analyses of surface rupture, teleseismic, strong motion and geodetic data all indicate a separation of the mainshock into subevents occurring on distinct fault segments (e.g. Reilinger et al., 2000; Tibi et al., 2001; Barka et al., 2002; Delouis et al., 2002). The western termination of the Izmit rupture is located offshore beneath the Sea of Marmara SE of the Prince Islands in direct vicinity to the Istanbul Metropolitan region (Bouchon et al., 2002; Özalaybey et al., 2002). Rupture propagation of the Izmit event almost

Published by Copernicus Publications on behalf of the European Geosciences Union.

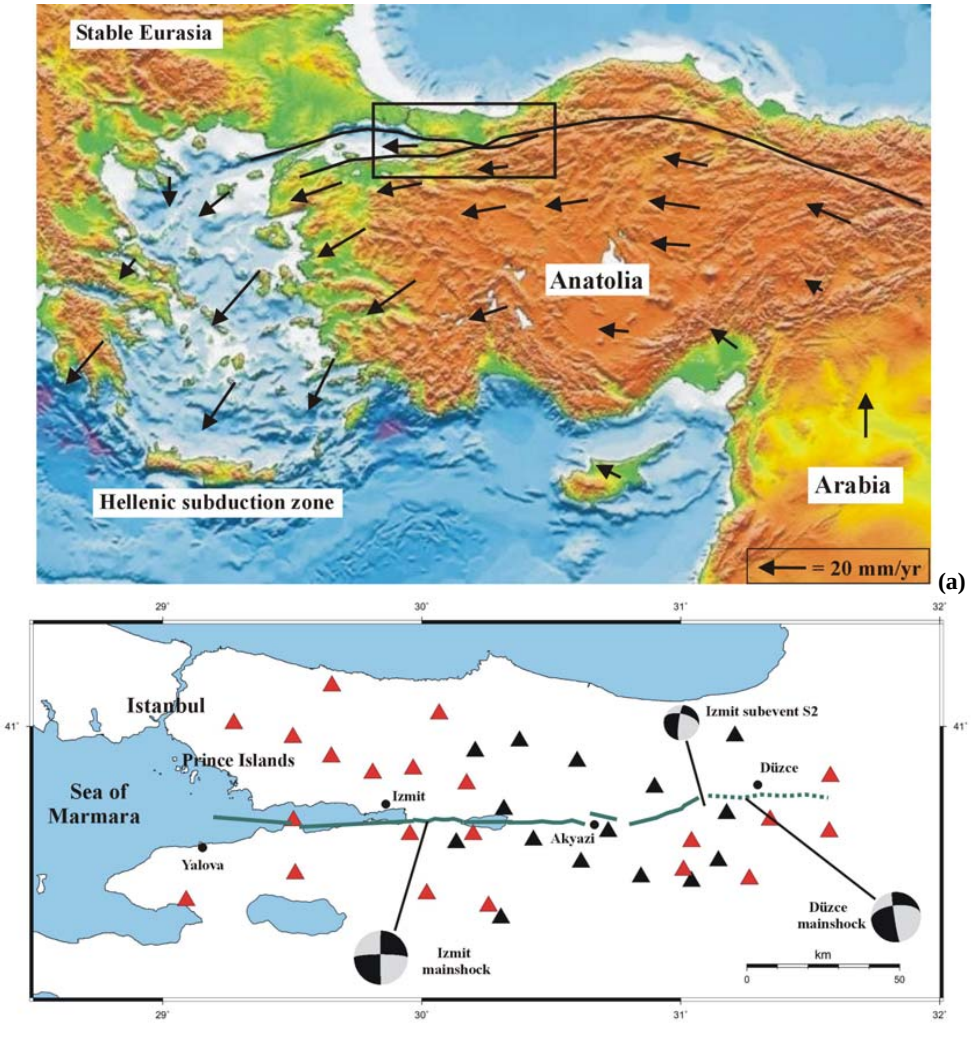

Fig. 1. **(a)** Location map of the Aegean-Anatolian region. Arrows indicate the GPS-derived horizontal velocity field (after McClusky et al., 2000) and their length scales with local velocities in mm/yr. The black line represents the North Anatolian Fault zone (simplified) extending from eastern Anatolia along northern Turkey and the Sea of Marmara towards the northern Aegean. The rectangle marks the study area including the rupture of the 1999 Mw=7.4 Izmit earthquake and is enlarged in (b). **(b)** Station distribution of the combined GTF and SABONET network that recorded the aftershock activity of the Izmit event (see text for details). Red and black triangles represent GFT and SABONET stations, respectively. Fault plane solutions are shown for the Izmit Mw=7.4 mainshock, its subevent S2 (Mw=6.7, Tibi et al., 2001) and for the Düzce Mw=7.1 mainshock. The bold green line indicates the surface rupture of the Izmit event after Barka et al. (2002) extrapolated for the offshore parts and the dotted green line marks the surface rupture of the Düzce event (Milkereit et al., 2000; Umutlu et al., 2004).

proceeded to the town of Düzce where a second large earthquake extended the rupture by another 50 km to the East only 87 days later (12 November 1999, Mw=7.1). Focal mechanisms of the Izmit mainshock, its major subevent (S2, Tibi et al., 2001) and the Düzce mainshock all indicate right-lateral strike-slip faulting with their nodal planes striking dominantly EW (Fig. 1b). This is in good agreement with the regional GPS-derived velocity field (McClusky et al., 2000).

In this study we present a catalog of Izmit aftershocks based on a 36-station seismic network that covered the entire rupture for a period of two months. We outline the data base that allowed generating the presumably most comprehensive Izmit aftershock catalog and highlight selected features where substantial scientific progress is expected based on this state of the art catalog.

2 The Izmit aftershock catalog

After the Izmit earthquake several temporary seismic networks were deployed along distinct parts the 140 km long rupture zone and surrounding areas resulting in numerous studies that examined the aftershock activity in detail (e.g. Örgülü and Aktar, 2001; Karabulut et al., 2002; Özalaybey et al., 2002; Ben-Zion et al., 2003; Aktar et al., 2004). Here we focus on recordings obtained by a 36-station seismic network that covered the entire Izmit rupture extending from the eastern Sea of Marmara towards the Düzce area. The aperture of the network is 180 km in EW direction along strike of the NAFZ and 70 km perpendicular to it resulting in an optimal coverage of the focal sphere for aftershocks occurring along the entire rupture (Fig. 1b).

A nucleus of the seismic network consisted of 15 stations that were in operation since 1996, the co-called SABONET (SApanca-BOlu NETwork, Milkereit et al., 2000). With the aim to monitor the Izmit aftershock activity at low magnitude-detection threshold the German Task Force for Earthquakes (GTF) that is based at the GeoForschungsZentrum Potsdam deployed additional 21 stations in the area within only four days after the mainshock (Zschau, Grosser, personal communication). The final deployment then contained 36 stations and was in operation for a period of 60 days. After GTF stations had been removed from the field the seismic monitoring was continued by SABONET. Figure 1b shows the distribution of GTF and SABONET stations indicated by red and black triangles, respectively. The average station spacing is 15 km. All stations were equipped with short-period seismometers of Type MARK L4-3D (eigenfrequency 1 Hz). Three stations were temporarily equipped with CMG-40T Guralp broadband sensors. Recorders from REFTEK (GTF) and Nanometrics (SABONET) served as data logger and were operated as stand-alone seismic units in the open field. Power supply was realized using rechargeable batteries and solar panels. SABONET stations allowed online transmission of data using telemetry.

Data were continuously recorded at 100 samples per second on three components. In this study we consider the time interval 24 August–9 November 1999. To evaluate the data, we ran a STA/LTA (short-term average/long-term average) trigger on the vertical component of each station as a first step. In general, events were selected if passing a coincidence trigger (>4 stations) combined with an algorithm neglecting events far outside the network. Possible appearance of simultaneous events at different locations along the rupture was considered by visual inspection of the seismic sections of all detected events and subsequent upgrade of the catalog. Phase onsets were picked manually. Absolute hypocenter determination for the joint GTF-SABONET network was performed using the HYPOCENTER earthquake location program (Lienert and Havskov, 1995) based on 104080 P-wave arrivals. An initial 1-D velocity model proposed by Özalaybey et al. (2002), was used to locate the

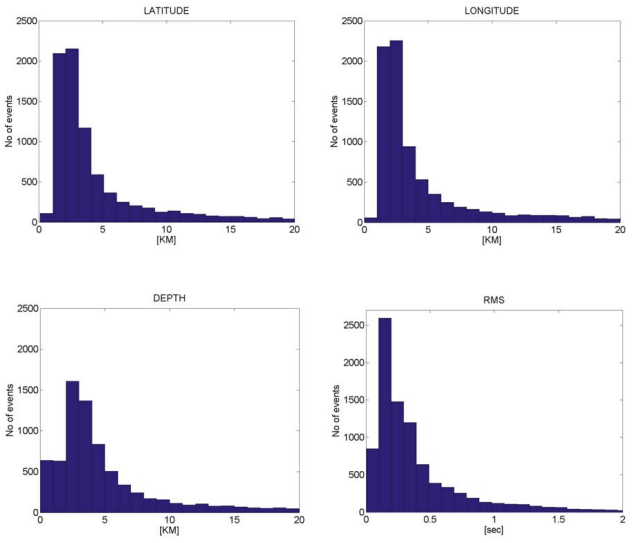

Fig. 2. Error distribution for events of the Izmit aftershock hypocenter catalog as determined from the combined GTF and SABONET network. The error is given in kilometer for latitude, longitude and depth, respectively, and in seconds for the root mean square (RMS) value. Approximately 70% percent of all events have a location error better than 5 km in all three directions and a RMS better than 0.3 s.

events. Applying the VELEST inversion code (Kissling et al., 1994) allowed refining the velocity model for the area of investigation and thus resulted in a significantly increased number of determined hypocenters (see Bulut et al., 2007, for details). As the starting depth is a sensitive parameter for the inversion we iteratively varied this parameter between 1 and 25 km and proceeded with the solution resulting in the lowest root mean square (RMS) value. Error bounds for the 7890 obtained hypocenter locations are plotted in Fig. 2 in terms of errors for latitude, longitude and depth, respectively, as well as the RMS value. The distribution of errors documents that ∼70% of the hypocenters have location errors less than 5 km in all three directions and RMS values below 0.3 s.

In addition to the catalog obtained from the joint GTF-SABONET network we added 2176 events recorded by SABONET after GTF stations were dismounted from the field. These hypocenters have similar location accuracy along most part of the rupture excluding the westernmost part below the Sea of Marmara (due to station distribution of SABONET, see Fig. 1b) and thus ensure a consistent continuous data base along the entire rupture east of the Sea of Marmara (see discussion below). The final catalogue of absolute Izmit aftershock hypocenter locations contains 10 066 events. For further analysis we restrict the catalog to events with location errors better than 5 km in both horizontal and vertical direction. This results in a total number of 7348 events that are plotted in map view and as depth section in Fig. 3.

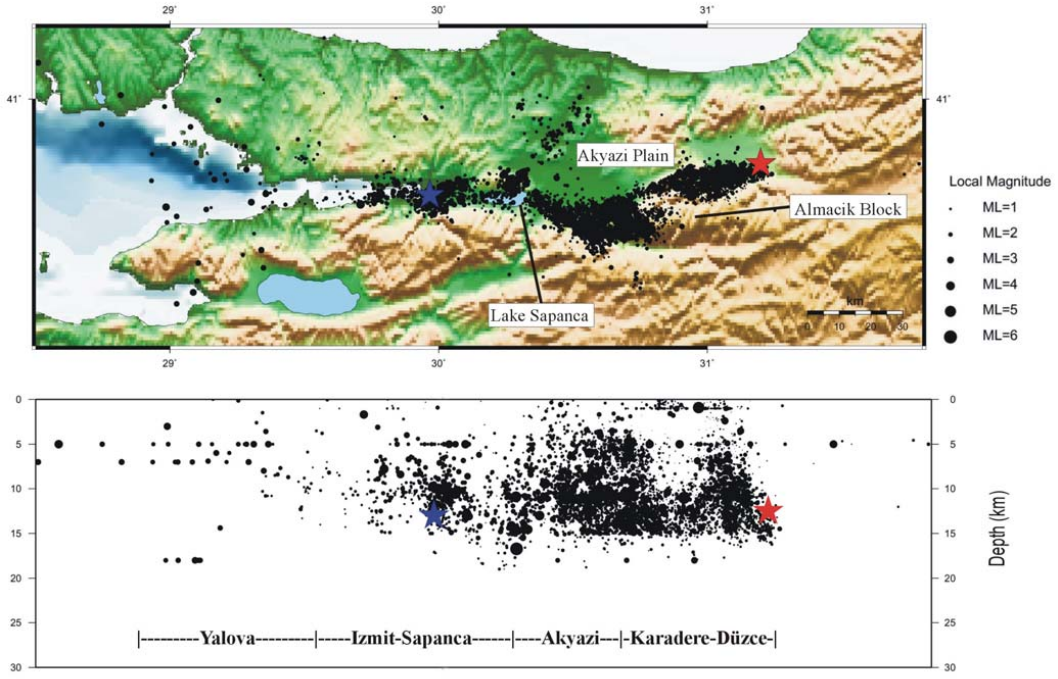

Fig. 3. Izmit aftershock hypocenter catalog in map view and as depth section. All 7348 events shown here have locations errors better than 5 km in all directions. A predominant activity is observed along the entire segment ruptured by the mainshock except the westernmost portion below the Sea of Marmara (see text for details) forming a 20 km wide band of activity. Two major clusters of activity are observed in the Akyazi and Karadere-Düzce areas. The majority of events occurred between 5 and 15 km depth. Blue and red stars indicate the location of the Izmit and Düzce hypocenter, respectively.

Local magnitudes were calculated following Baumbach et al. (2003) who developed a procedure to determine M_l for NW Turkey that was refined by Bindi et al. (2007) based on an updated attenuation curve and refined station corrections. The procedure basically involves an automatic estimation of M_l for all events at each station deconvolving the traces to synthetic Wood-Anderson torsion seismograms using instrument response and maximum horizontal peak amplitudes. Figure 4 shows the magnitude-frequency distribution for the Izmit aftershock catalog as plotted in Fig. 3. The overall magnitude threshold of completeness is Mc=1.1 and the largest event had a magnitude of 5.8. Plotting Mc with time reveals a decreased magnitude threshold during the last two weeks after GTF stations were dismounted which is explained by technical reasons caused by a different data evaluation procedure (see also Gorgün et al., 2007).

3 Spatial distribution of aftershocks

The spatial distribution of Izmit aftershock hypocenters as plotted in Fig. 3 stresses that events occurred along the entire ruptured NAFZ segment forming a 20 km wide band of seismicity with a predominant activity observed towards the eastern part. This was also observed earlier based on aftershock catalogs with a somewhat larger magnitude threshold (e.g. Aktar et al., 2004). Seismicity defines four distinct areas that exhibit varying levels of activity and that coincide with individual fault segments observed from coseismic rupture (see e.g. Barka et al., 2002), namely the Yalova, Izmit-Sapanca, Akyazi and Karadere-Düzce segments from West to East (Fig. 3). The highest level of seismic activity is observed in the Akyazi and Karadere-Düzce areas. The eastern termination of aftershock activity reflects a sharp steeply dipping boundary exactly where the Düzce mainshock initiated 87 days after the Izmit event (Milkereit et al., 2000; Umutlu et al., 2004; see red star in Fig. 3). Most hypocenters are concentrated between 5 and 15 km depth. The highest density of events is observed below the Akyazi Plain narrowing towards the West in good correspondence with the vertically oriented coseismic slip zone in this area. Further to the West, the Izmit-Sapanca segment exhibits dominant activity around the hypocenter of the Izmit mainshock (blue star in Fig. 3).

The westernmost segment below the eastern Sea of Marmara reflects only minor seismic activity in our catalog. We recall that the data set was restricted to events with location accuracy better than 5 km. The initial catalog including also events with somewhat larger error bounds towards the western end that are diffusely distributed indicating a branching of seismicity. However, due to the somewhat sparser coverage of our network in this area compared to the remaining

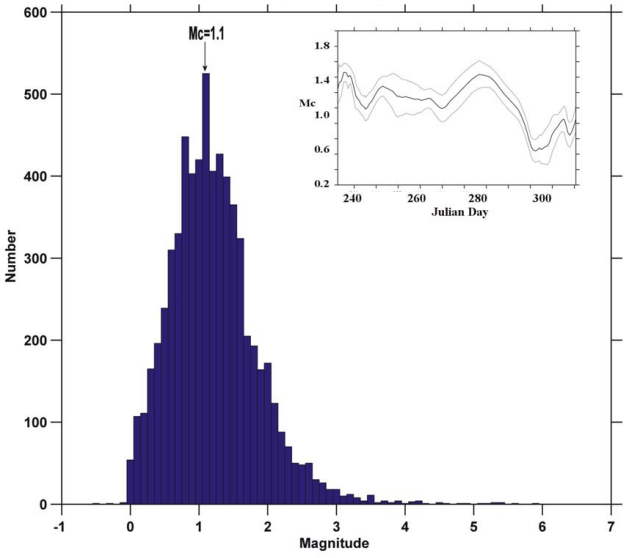

Fig. 4. Magnitude frequency of the Izmit aftershock hypocenter catalog as shown in Fig. 3. The magnitude threshold of completeness of the joint GTF and SABONET network is Mc=1.1. Events down to magnitudes as low as 0 are located and the largest magnitude contained in the catalog is 5.8. The inset shows the temporal evolution of Mc during the Izmit aftershock sequence. Stable values for Mc are observed throughout the first ∼55 days. A significant decrease of Mc is observed after Julian day 290 which is due to technical reasons (see Görgün et al., 2007[1], for details).

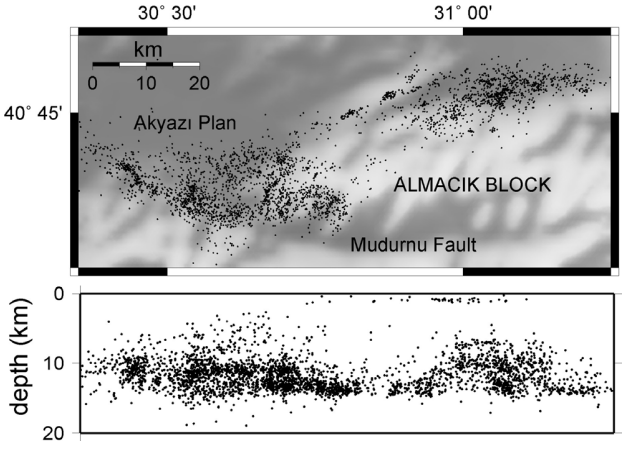

Fig. 5. Relocated hypocenter catalog of Izmit aftershocks in the Akyazi and Karadere-Düzce area (western half of the rupture). Relative location accuracy improved by a factor of 6 compared to absolute hypocenters shown in Fig. 3 and allows to identify internal structures within the seismically active area. Several planes as well as cloud-type distribution of activity down to the resolved scale of 300 and 400 m for horizontal and vertical direction, respectively, is observed in both clusters (see text for details).

part of the Izmit rupture we abstain from further analysis of the seismicity in the Yalova area and refer to Karabulut et al. (2002) and Aktar et al. (2004) who operated denser networks in this area. Interestingly, Karabulut et al. (2002) observe a branching of the NAFZ into several streaks of activity below the easternmost Sea of Marmara which was also obtained for this area from spatial clustering of similar aftershock focal mechanisms (Bohnhoff et al., 2006).

4 Relocation of Izmit aftershocks

In order improve the spatial resolution within the seismically active areas we relocated the aftershocks by applying the well-established double-difference earthquake relocation algorithm (Waldhauser and Ellsworth, 2000). Previous studies showed that the method is successful not only for understanding the pattern of internal structures at small scale which are left hidden in absolute located earthquake catalogs but also for addressing seismotectonic aspects in seismically active regions. A total of 4696 aftershocks of the Akyazi/Düzce-Karadere clusters fulfilled the required criteria and were relocated based on relative travel-time data and cross-correlation analysis (see Bulut et al., 2007, for details). The relocated catalog of Izmit aftershocks for the Akyazi and Karadere-Düzce area reveals a number of structural features not identified from the absolute locations (see Fig. 5). A clear distinction into narrow planes of activity and more cloud-like distributions are observed in direct vicinity. The cloud-type distribution is justified down to the resolved spatial accuracy of 400 (vert.) m 300 m (hor.), i.e. features smaller than that might exist but are not resolved. From the map view in Fig. 5 the existence of two main clusters of activity is clearly confirmed. The majority of events are observed between 6 and 16 km depth and only a smaller number occurred near the surface in the Karadere-Düzce area. Thus, the overall hypocentral distribution as identified from absolute hypocenters (Fig. 3) is confirmed but its internal structure is significantly refined. Moreover, the depth distribution was found being stable against different velocity models formerly proposed for the region (Bulut et al., 2007).

5 Discussion and conclusion

The Akyazi cluster extends from east of the Sapanca Lake towards the western Almacik Block covering the Akyazi Plain to some extent (Fig. 5). The Akyazi Plain itself reflects a local topographical depression subsided by ∼500 m. Aftershocks cluster predominantly at its southern part where the NAFZ forms a triple junction between with the Karadere and Mudurnu faults. The area between Lake Sapanca and the Almacik Block is interpreted to represent a small pull-apart basin (Bohnhoff et al., 2006) similar to the Lake Sapanca, the Izmit Bay and the somewhat larger Sea of Marmara (Armijo et al., 1999). Inside the activity cluster two predominant linear features are observed: In the SW a prominent N130° E

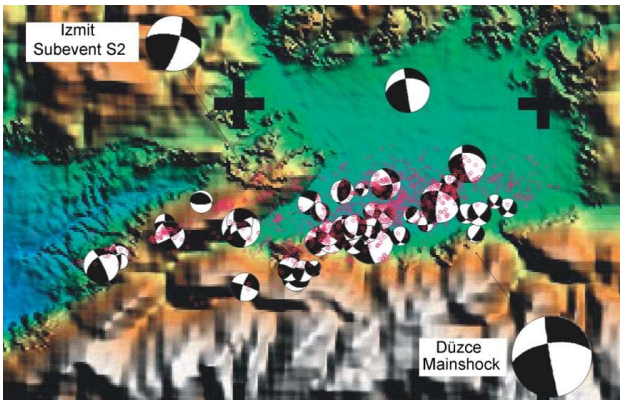

Fig. 6. Karadere-Düzce area representing the easternmost part of the Izmit rupture. Topography was plotted after Fielding et al. (1999). Red dots indicate relocated hypocenters as shown in Fig. 5 that are subdivided into a narrow band of activity representing the down-dip extension of the Karadere fault in the west and a cloud of activity without internal structure down to the resolved scale of 400 m in the East. Fault plane solutions are from Bohnhoff et al. (2006) and include the four largest aftershocks of this segment, the Izmit subevent S2 (Tibi et al., 2001) and the Düzce mainshock. These six events all have an almost identical focal mechanism reflecting slip on an EW trending steeply northward dipping fault plane. This part of the NAFZ is interpreted to reflect a typical example for a fault barrier that was activated by the Izmit mainshock and re-ruptured and extended by the Düzce event after 87 days.

trending plane of hypocenters is observed forming the westward extension of the Mudurnu fault where a M>7 earthquake occurred in 1967 (Ambraseys and Zatopek, 1969). The western termination of that rupture intersects with the eastern end of the plane formed by Izmit aftershocks. We conclude that the Mudurnu fault as one major branch of the NAFZ did not built-up a sufficient slip deficit since the 1967 mainshock to be reactivated by the Izmit event. The second feature observed within the Akyazi cluster is a NNE-SSW trending plane at the southwestern boundary of the Almacik Block. This plane is dipping to the WNW at an angle of ∼60° and its orientation is in good correspondence with the high number of EW-extensional normal faulting events observed in this area. It is therefore likely to represent the fault plane of one or more of the larger aftershocks of this area. In general this highlights the benefit of generating high-resolution aftershock catalogs with regard to discrimination of nodal from auxiliary planes of focal mechanisms.

The Karadere-Düzce cluster covers the easternmost 35 km of the Izmit rupture being located north of the Almacik Block. Its most prominent planar structure is a 25 km long N65° E trending plane that dips at an angle of 65° to the NNW. This plane is interpreted to represent the down-dip extension of the Karadere fault that hosted about 1 m of right-lateral coseismic slip during the Izmit event and is identified by a narrow topographical trace at the surface. East of this plane a more diffuse distribution of aftershocks is observed with an eastward dipping termination of activity exactly where the Izmit rupture stopped and where the Mw=7.1 Düzce mainshock initiated its rupture. The Düzce event ruptured bi-directionally, i.e. re-ruptured parts of the Karadere-Düzce segment and extended the rupture to the East (Umutlu et al., 2004).

Estimates of average coseismic fault slip for the Izmit mainshock vary between 2.5 m (e.g. Tibi et al., 2001) and 2.9 m (Bouchon et al., 2002) from inversion of teleseismic data and records of near-fault accelerometers, respectively. Maximum slip at the surface was observed in the Sapanca-Akyazi area reaching about 5–6 m (Barka et al., 2002; Bouchon et al., 2002). The direction of slip corresponds well with the overall horizontal GPS-derived 25 mm/yr westward motion of the Anatolian block with respect to Eurasia in this area (McClusky et al., 2000). Analyses of surface rupture, teleseismic, strong motion and geodetic data all indicate a separation of the mainshock into subevents occurring on distinct fault segments (e.g. Reilinger et al., 2000; Tibi et al., 2001; Barka et al., 2002; Delouis et al., 2002). The Akyazi Plain is consistently identified as an area of reduced slip.

Focussing on the temporal evolution of coseismic slip Delouis et al. (2002) presented a detailed source-time function of the Izmit mainshock. The first ∼15 s of rupture included the largest portion of coseismically released energy being associated with the slip maximum in the Izmit-Sapanca area. After 15 s of "co-seismic silence" a second significant portion of slip occurred that was correlated with a so-called Izmit subevent S2. The location of S2 was further to the East on the Karadere-Düzce segment. Its magnitude was calculated as Mw=6.7 on a fault plane that represents slip on a EW trending steeply northward dipping fault plane (Tibi et al., 2001; see Fig. 6) was determined. Interestingly, the focal mechanism of Izmit subevent S2 is highly similar to the focal mechanisms of the four largest (M>4) aftershocks on the Karadere-Düzce segment of which three occurred within the first six hours after the mainshock. These five events all occurred below the Düzce Basin, a small-scale local depression in topography where a diffuse distribution of aftershock activity was observed down to the resolved scale of 300 m and 400 m for horizontal and vertical directions, respectively. Moreover the fault plane solutions of these events are almost identical to the fault plane solution of the Düzce mainshock. We interpret this segment between the Karadere fault and the eastern rupture termination of the Izmit event as a classical example of a seismic barrier where accelerated seismic activity was observed after the Izmit event. There, the larger events all occurring on different parts of the same fault patch that then ruptured in a concerted fashion after a period of almost three months (the Mw=7.1 Düzce mainshock) extending along the entire length of this barrier and furthermore by another 20 km to the East.

Acknowledgements. We thank the German Task Force for Earthquakes hosted at GeoForschungsZentrum in Potsdam and especially J. Zschau and H. Grosser for providing the continuous seismic recordings obtained by the GTF network after the 1999 Izmit earthquake and E. Günther, H. Grosser, S. Zünbül, and S. Karakisa for maintenance of the network. Furthermore we thank D. Bindi and S. Parolai for excellent collaboration and magnitude determination.

Edited by: P. Fabian
Reviewed by: two anonymous referees

References

Aktar, M., Özalaybey, S., Ergin, M., Karabulut, H., Bouin, M., P., Tapirdamaz, C., Biçmen, F., Yörük, A., and Bouchon, M.: Fault Zone Heterogeneity and Variations of Seismicity Parameters across 1999 Ýzmit-Düzce Earthquake Sequence, Tectonophysics, 391, 325–334, 2004.

Ambraseys, N. N. and Zatopek, A.: The Mudurnu Valley, West Anatolia, Turkey, earthquake of 22 July 1967 , Bull. Seismol. Soc. Am., 59(2), 521–589, 1969.

Ambraseys, N. N.: Some characteristic features of the North Anatolian fault zone into the north Aegean, Tectonophysics, 9, 143–165, 1970.

Armijo, R., Meyer, B., Hubert, A., and Barka, A.: Westward propagation of the North Anatolian Fault into the northern Aegean: timing and kinematics, Geology, 27, 267–270, 1999..

Barka, A.: The North Anatolian Fault, Ann. Tectonicae, 6, 164–195, 1992.

Barka, A.: The 17 August Izmit earthquake, Science, 285, 1858–1859, 1999.

Barka, A., Akyuz, H. S., Altunel, E., et al.: The Surface Rupture and Slip Distribution of the 17 August 1999 Izmit Earthquake (M 7.4), North Anatolian Fault, Bull. Seism. Soc. Am., 92(1), 43–60, 2002.

Baumbach, M., Bindi, D., Grosser, H., Milkereit, C., Parolai, S., Wang, R., Karakisa, S., Zünbül, S., and Zschau, J.: Calibration of a Ml scale in the Northwestern Turkey from 1999 Izmit aftershocks, Bull. Seism. Soc. Am., 93(5), 2289–2295, 2003.

Ben-Zion, Y., Peng, Z., Okaya, D., Seeber, L., Armbruster, J. G., Michael, A. J., Baris, S., and Aktar, M.: A shallow fault-zone structure illuminated by trapped waves in the Karadere-Düzce branch of the North Anatolian Fault, western Turkey, Geophys. J. Int., 152, 699–717, 2003.

Bindi, D., Parolai, S., Görgün, E., Grosser, H., Milkereit, C., Bohnhoff, M., and Durukal, E.: Ml Scale in Northwestern Turkey from 1999 Izmit aftershocks: Updates, Bull. Seism., Soc. Am., 97, 331–338, 2007.

Bohnhoff, M., Grosser, H., and Dresen, G.: Strain Partitioning and Stress Rotation at the North Anatolian Fault Zone from aftershock focal mechanisms of the 1999 Izmit Mw=7.4 Earthquake, Geophys. J. Int., 166, 373–385, 2005.

Bouchon, M., Töksöz, M. N., Karabulut, H., Bouin, M.-P., Dietrich, M., Aktar, M., and Edie, M.: Space and Time Evolution of Rupture and Faulting during the 1999 Izmit (Turkey) Earthquake, Bull. Seism. Soc. Am., 92(1), 256–266, 2002.

Bulut, F., Bohnhoff, M., Aktar, M., and Dresen, G.: Characterization of aftershock-fault plane orientations of 1999 Izmit (Turkey) earthquake using high-resolution aftershock locations, Geophys. Res. Lett., 34, doi:2007GL031154, in press 2007.

Delouis, B., Giardini, C., Lundgren, P., and Salichon, J.: Joint inversion of InSAR, GPS, Teleseismic, and Strong-Motion Data for the Spatial and Temporal Distribution of Earthquake slip: Application to the 1999 Izmit Mainshock, Bull. Seism. Soc. Am., 92(1), 278–299, 2002.

Fielding, E. J., Wright, T. J., Parsons, B. E., England, P. C., Rosen, P. A., Hensley, S., and Bilham, R.: Topography of northwest Turkey from SAR interferometry: applications to the 1999 Izmit earthquake geomorphology and coseismic strain, EoS Trans., Am. Geophys. Union, 80, 46, F762, 1999.

Hubert-Ferrari, A., Barka, A., Jacques, E., Nalbant, S. S., Meyer, B., Armijo, R. Traponnier, P., and King, G. C. P.: Seismic hazard in the Marmara Sea following the 17 August 1999 Izmit earthquake, Nature, 404, 269–273, 2000.

Hubert-Ferrari, A., Armijo, R., King, G., and Meyer, B.: Morphology, displacement and slip rates along the North Anatolian Fault, Turkey, J. Geophys. Res., 107(B10), 2235, doi:10.1029/2001JB000393, 2002.

Karabulut, H., Bouin, M.-P., Bouchon, M., Dietrich, M., Cornou, C., and Aktar, M.: The seismicity in the Eastern Marmara Sea after the 17 August 1999 Izmit Earthquake, Bull. Seismol. Soc. Am., 92(1), 387–393, 2002.

Kissling, E., Ellsworth, W. L., Eberhart-Philipps, D., and Kradolfer, U.: Initial reference models in local earthquake tomography, J. Geophys. Res., 99, 19 635–19 646, 1994.

Lienert, B. R. and Havskov, J.: HYPOCENTER 3.2 -A computer program for locating earthquakes locally, regionally and globally, Seis. Res. Lett., 66, 26–36, 1995.

McClusky, S., Balassanian, S., Barka, A., et al.: Global Positioning System constraints on plate kinematics and dynamics in the eastern Mediterranean and Caucasus, J. Geophys. Res., 105, 5695–5719, 2000.

Milkereit, C., Zünbül, S., Karakisa, S., Iravul, Y., Zschau, J., Baumbach, M., Grosser, H., Günther, E., Umutlu, N., Kuru, T., Erkul, E., Klinge, K., Ibs von Seht, M., Karahan, A.: Preliminary aftershock analysis of the Mw=7.4 Izmit and Mw=7.1 Düzce earthquake in western Turkey, in: The 1999 Izmit and Düzce Earthquakes: Preliminary Results, edited by: Barka, A., Kozaci, O., and Akyüz, S., Istanbul Technical University, ISBN 975-561-182-7, 179–187, 2000.

Muller, J. R. and Aydin, A.: Using mechanical modelling to constrain fault geometries proposed for the northern Marmara sea, J. Geophys. Res., 110, B03407, doi:10.1029/2004JB003226, 2005.

Örgülü, G. and Aktar, M.: Regional Moment Tensor Inversion for Strong Aftershocks of the August 17, 1999 Izmit Earthquake (Mw=7.4), Geophys. Res. Lett., 28(2), 371–374, 2001.

Özalaybey, S., Ergin, M., Aktar, M. Tapirdamaz, C., Bicman, F., and Yörük, A.: The 1999 Izmit Earthquake Sequence in Turkey: Seismological and Tectonic Aspects, Bull. Seism. Soc. Am., 92(1), 376–386, 2002.

Reilinger, R., Toksöz, N., McClusky, S., and Barka, A.: The 1999 Izmit, Turkey, earthquake was no surprise, GSA Today, 10(1), 1–6, 2000.

Stein, R. S., Barka, A., and Dieterich, J. H.: Progressive failure of the North Anatolian fault since 1939 by earthquake stress triggering, Geophys. J. Int., 128, 594–604, 1997.

Straub, C., Kahle, H.-G., and Schindler, C.: GPS and geologic estimates of the tectonic activity in the Marmara Sea region, NW Anatolia, J. Geophys. Res., 102, 27 587–27 601, 1997.

Tibi, R., Bock, G., Xia, Y., Baumbach, M., Grosser, H., Milkereit, C., Karakisa, S., Zünbül, S., Kind, R., and Zschau, J.: Rupture processes of the 1999 August 17 Izmit and November 12 Düzce (Turkey) earthquakes, Geophys. J. Int., 144, F1–F7, 2001.

Töksöz, M. N., Shakal, A. F., and Michael, A. J.: Space-time migration of earthquakes along the North Anatolian Fault and seismic gaps, PAGEOPH, 117, 1258–1270, 1979.

Umutlu, N., Kuketsu, K., and Milkereit, C.: The rupture process during the 1999 Düzce, Turkey, earthquake from joint inversion of teleseismic and strong-motion data, Tectonophysics, 391, 315–324, 2004.

Waldhauser, F. and Ellsworth, W. L.: A double-difference earthquake location algorithm: Method and application to the northern Hayward fault, Bull. Seism. Soc. Am., 90, 1353–1368, 2000.